Modeling the Flux of Muonic Neutrinos in Spatial & Temporal Coincidence with Prompt Gamma-Ray Emission from Discrete BATSE GRBs Using Fireball Phenomenology & AMANDA Observations

Michael Stamatikos† for the AMANDA Collaboration

†Department of Physics, University of Wisconsin, Madison, WI, USA

ABSTRACT: Neutrino-based astronomy provides a new window on the most energetic processes in the universe. The discovery of high-energy ($E_\nu = 10^{14}$ eV) neutrinos from gamma-ray bursts (GRBs) would confirm hadronic acceleration in the relativistic GRB-wind, validate the phenomenology of the canonical fireball model and possibly reveal an acceleration mechanism for the highest energy cosmic rays. The Antarctic Muon and Neutrino Detector Array (AMANDA) is the world's largest operational neutrino telescope, with a PeV muon effective area (averaged over zenith angle) ~ 50,000 m². AMANDA uses the natural ice at the geographic South Pole as a Cherenkov medium and has been successfully calibrated on the signal of atmospheric neutrinos. Contrary to previous diffuse searches, we describe an analysis based upon confronting AMANDA observations of individual GRBs, adequately modeled by fireball phenomenology, with the predictions of the canonical fireball model. The expected neutrino flux is directly derived from the fireball model description of the prompt GRB photon energy spectrum, whose spectral fit parameters are described by the Band Function.

The expected neutrino event rate is a function of the distribution of each individual burst in spectroscopically observed or best-estimated redshift. Strict spatial and temporal constraints (based upon satellite detection), in conjunction with selection criteria (optimized for sensitivity) will be leveraged to realize a nearly background-free search. This work augments the primary science goals of GRB satellite detectors such as BATSE, by providing a necessary complementary neutrino analysis, which is readily applicable to future missions such as Swift and GLAST. Coincident neutrino searches using Swift GRBs would work in conjunction with Swift's key projects to enhance Swift's science return without imposing additional demands upon mission resources. Future work involves a natural extension to IceCube (the next generation km-scale neutrino telescope), whose superior sensitivity coupled with the high quality and completeness of Swift and GLAST data may help constrain (or in some cases rule out) certain GRB models. In this manner, AMANDA and IceCube will help maximize neutrino astronomy's contribution to the study of GRBs, even in the case of non-detection.

I. Theoretical Foundations: Fireball Phenomenology, Observables & The GRB-Neutrino Connection

Figure 1: Overview of Fireball Phenomenology[1]

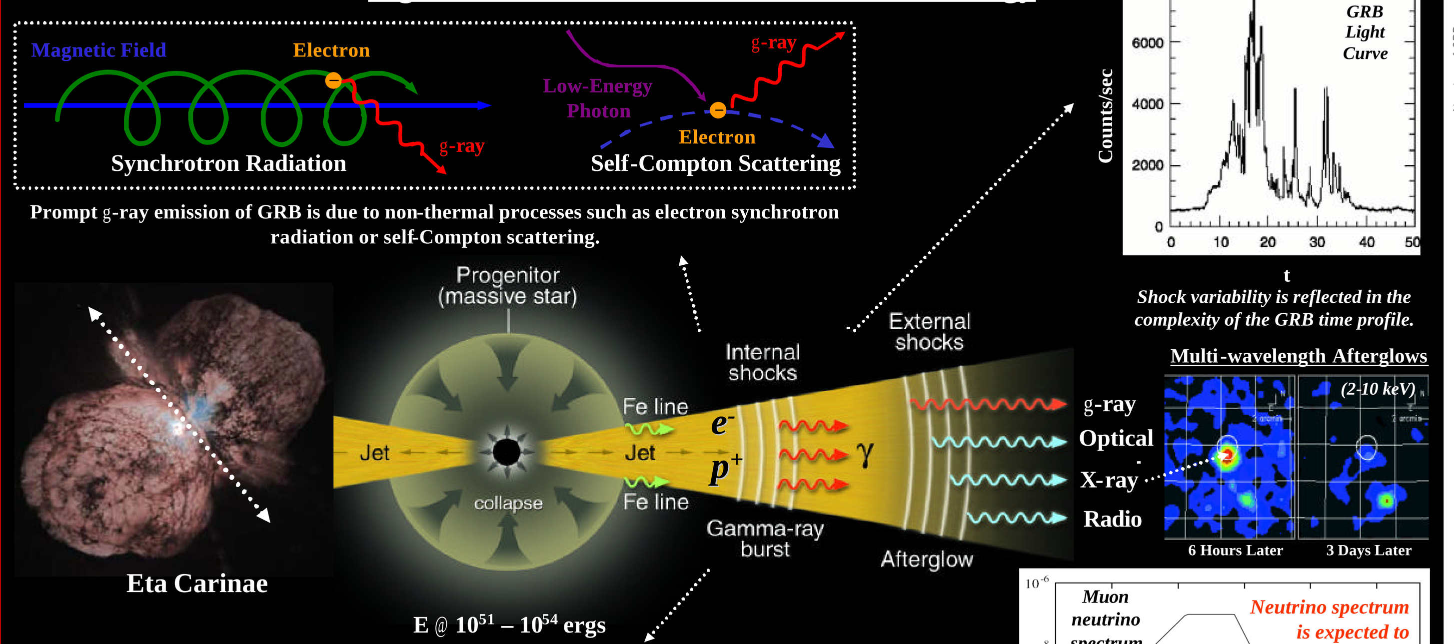

$$\text{If } E^{p\gamma}_{cm} > E^{Th}_{\Delta^+} \Rightarrow p^+ + \gamma \rightarrow \Delta^+ \rightarrow (n) + \pi^+ \rightarrow \nu_\mu + \mu^+ \rightarrow \nu_\mu + e^+ + \nu_e + \bar{\nu}_\mu$$

Photomeson interactions involving relativistically ($\Gamma \approx 300$) shock-accelerated protons ($E_p \geq 10^{16}$ eV) and synchrotron gamma-ray photons ($E_\gamma \approx 250$ keV) in the fireball wind yield high-energy muonic neutrinos ($E_\nu \approx 10^{14} – 10^{15}$ eV).

R < 10⁸ cm

R ≤ 10¹⁴ cm, T @ 3 x 10³ seconds

R ≤ 10¹⁸ cm, T @ 3 x 10¹⁶ seconds

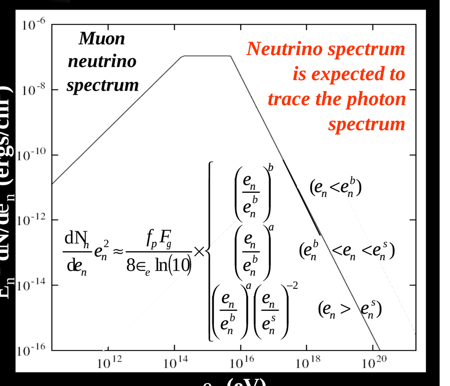

$$\frac{dN_\nu}{d\epsilon_\nu}\epsilon_\nu^2 \approx \frac{f_\pi F_\gamma}{8\epsilon_e \ln(10)} \times \begin{cases} \left(\frac{\epsilon_\nu}{\epsilon_\nu^b}\right)^{\beta} & (\epsilon_\nu < \epsilon_\nu^b) \\ \left(\frac{\epsilon_\nu}{\epsilon_\nu^b}\right)^{\alpha} & (\epsilon_\nu^b < \epsilon_\nu < \epsilon_\nu^s) \\ \left(\frac{\epsilon_\nu}{\epsilon_\nu^b}\right)^{\alpha}\left(\frac{\epsilon_\nu}{\epsilon_\nu^s}\right)^{-2} & (\epsilon_\nu > \epsilon_\nu^s) \end{cases}$$

$E^{p\gamma}_{cm} \equiv$ Center of mass energy for pγ interaction & $E^{Th}_{\Delta^+} \equiv$ Threshold energy for producing Δ^+

Minimum Proton Energy‡ (e_p) **Coincident Neutrino Energy‡ (e_ν)** ‡ *In Laboratory Frame*

$$\epsilon_p \geq \left[(1.4\times10^{16})\frac{\Gamma_{2.5}^2}{\epsilon_{\gamma,MeV}}\right]\text{eV} \sim 10^{16}\text{ eV} \qquad \Gamma_{2.5} \equiv \frac{\Gamma}{10^{2.5}}$$

$$\epsilon_\nu = \frac{1}{4}\langle x_{p^+\rightarrow\pi^+}\rangle\epsilon_p \Rightarrow \epsilon_\nu \approx 10^{14} - 10^{15}\text{ eV}$$

$$f_\pi \approx \langle x_{p^+\rightarrow\pi^+}\rangle \approx 0.2\frac{L_{\gamma,52}}{\Gamma_{2.5}^4 t_{v,-2}\epsilon^b_{\gamma,MeV}} \equiv \text{proton efficiency}.$$

Neutrino Break Energies‡ (e_ν^b, $e_{\nu_\mu}^s$)

$$\epsilon_\nu^b \geq \left[\frac{7\times10^{14}}{(1+z)^2}\frac{\Gamma_{2.5}^2}{\epsilon^b_{\gamma,MeV}}\right]\text{eV} \sim 700\text{ TeV} \qquad \epsilon^s_{\nu_\mu} = \left[\frac{10^{17}}{1+z}\sqrt{\frac{\epsilon_e}{\epsilon_B}}\frac{\Gamma_{2.5}^4 t_{v,-2}}{\sqrt{L_{\gamma,52}}}\right]\text{eV} \sim 10\text{ PeV}$$

$\epsilon_e \equiv$ Fraction of internal energy converted to e⁻ & $\epsilon_B \equiv$ Fraction of internal energy converted to B; $t_{v,-2} \equiv \frac{t_v}{10^{-2}}$ sec $\equiv$ Fluctuations in GRB γ-spectra & $L_{\gamma,52} \equiv \frac{L_\gamma}{10^{52}}$ ergs/sec $\equiv$ Observed GRB luminosity

Figure 2: The Burst and Transient Source Experiment (BATSE)

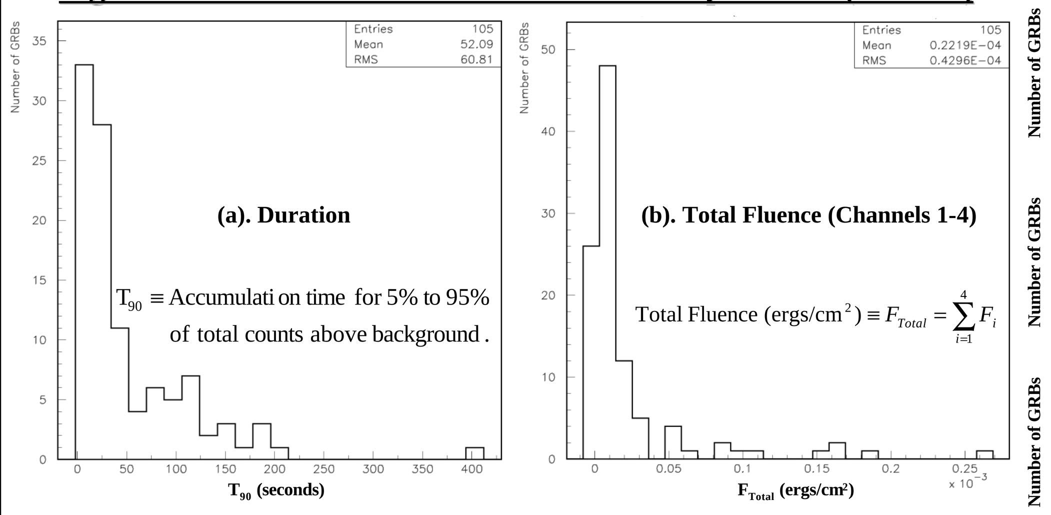

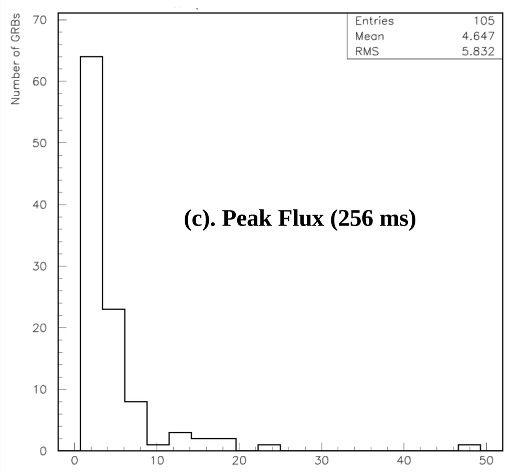

(d). Sky plot of 105 BATSE GRBs Utilized in Discrete AMANDA Analysis

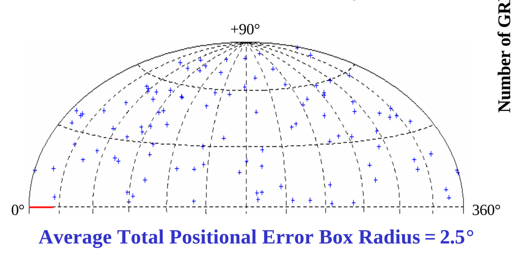

Average Total Positional Error Box Radius = 2.5°

Selection Criteria for 105 BATSE GRB Sample

Truncated Julian Dates (TJD) 10543-10767, 10859-11160, 11219-11493 & 11587-11683 (1997-2000)
Declination = 0°(Northern hemisphere localization)
Duration ($T_{90} \pm \sigma_{T_{90}}$) = 2 s (i.e. Long GRBs)
Peak Flux = 1.5 photons·(cm²·s)⁻¹

The distributions of the observables in figures 2a -2d, were generated from the values given in [2]. In conjunction with the fluence and duration, the spectroscopic redshift (figure 3a) is used to determined the burst luminosity (see equation 1). When not observed, the redshifts for this sample were estimated via either variability [3], lag [4], or peak energy *(i.e. E_P, the energy at which the energy flux per logarithmic energy band peaks)* [5] luminosity relations (see figures 3b -3d).

Figure 3: Comparison of Redshift Distributions

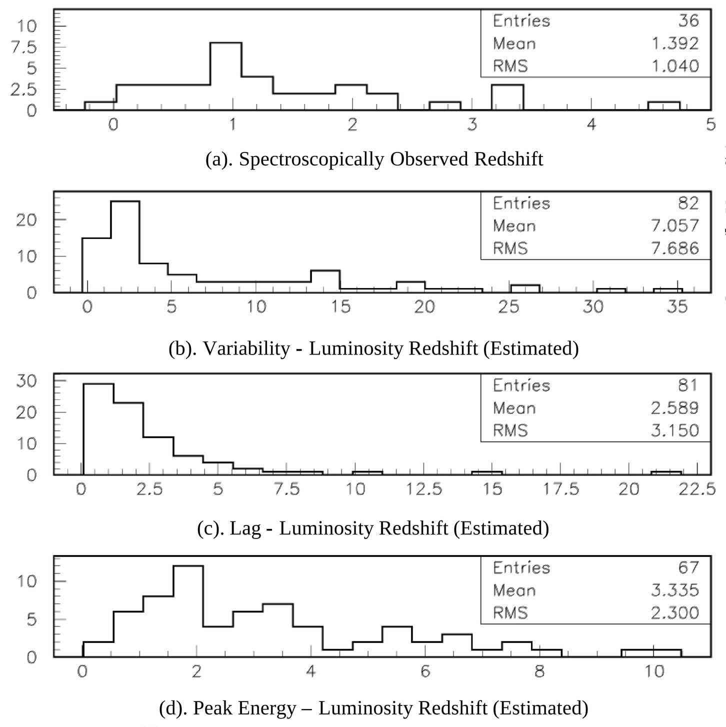

$$L_\gamma = \frac{F_\gamma 4\pi d^2}{T_{90}} \qquad \text{Where: } d = \frac{c}{H_o}\int_0^z \frac{dz'}{\left[\Omega_\Lambda + \Omega_M(1+z')^3\right]^{1/2}} \tag{1}$$

$$N_E(E) = \begin{cases} A\left(\frac{E}{100\text{ keV}}\right)^{\alpha} e^{\left(-\frac{E}{E_o}\right)} & (\alpha-\beta)E_o \geq E \\ A\left[\frac{(\alpha-\beta)E_o}{100\text{ keV}}\right]^{(\alpha-\beta)} e^{(\beta-\alpha)}\left(\frac{E}{100\text{ keV}}\right)^{\beta} & (\alpha-\beta)E_o \leq E \end{cases} \tag{2}$$

The prompt photon energy spectrum can be adequately described (independently of physical emission models) by the Band function [6] (see equation 2, figure 4a & 4b), as long as the spectral fit parameters are allowed to vary *(i.e. there are no universal set of parameters)*. Figures 4c - 4f illustrate the distribution of the peak spectral fit parameters [6] for the bursts used in this analysis. The importance of properly fitting discrete photon energy spectra can be seen in the analysis of GRB 941017 [7].

Figure 4: Distribution of Band Peak Energy Spectral Fit Parameters[6]

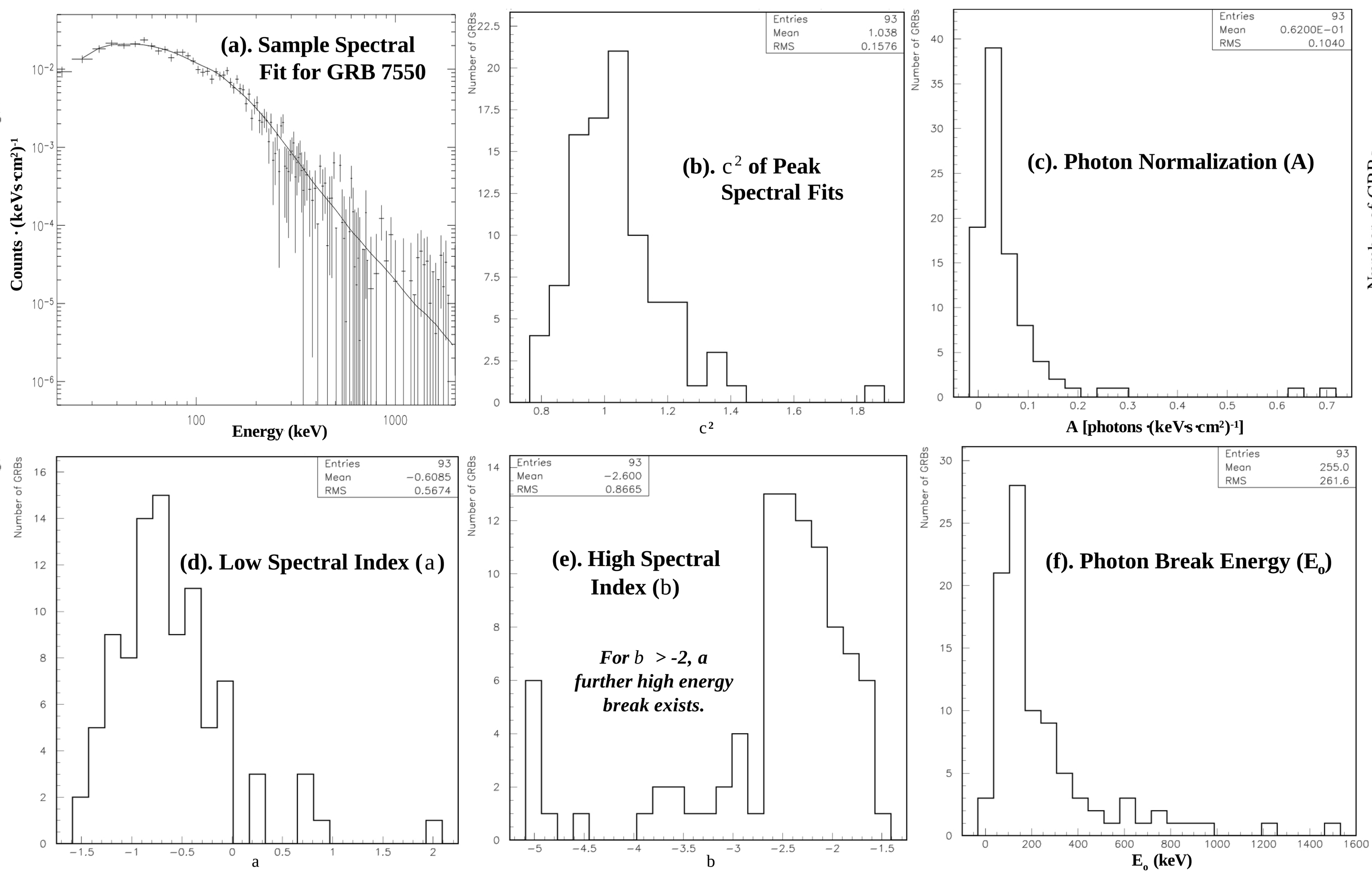

In the framework of the canonical fireball phenomenology (see figure 1), GRB electromagnetic observables such as duration, fluence, and luminosity (via redshift) coupled with the photon energy spectral fit parameters are required to parameterize the normalization, break energies and spectral slopes of the neutrino spectra [1] in spatial and temporal coincidence with the prompt γ-ray emission. Since these observables vary from burst to burst, the expected neutrino energy spectrum is also uniquely defined for each discrete GRB. As can be seen from the above distributions (figures 2 – 4), the parameters can differ significantly from their canonical (averaged) values. Hence, both the normalization and shape of a discrete neutrino energy spectrum can vary significantly from an averaged (diffuse) [8] construction, which directly affects the event rate expectation (see figure 5) and sensitivity optimization of coincident search analyses (respectively) as performed by Cherenkov telescopes such as AMANDA or IceCube. The focus of this ongoing analysis, is to investigate the effects of individual neutrino spectra for discrete GRB observations with AMANDA and eventually IceCube.

Figure 5: Neutrino Event Rates[1]

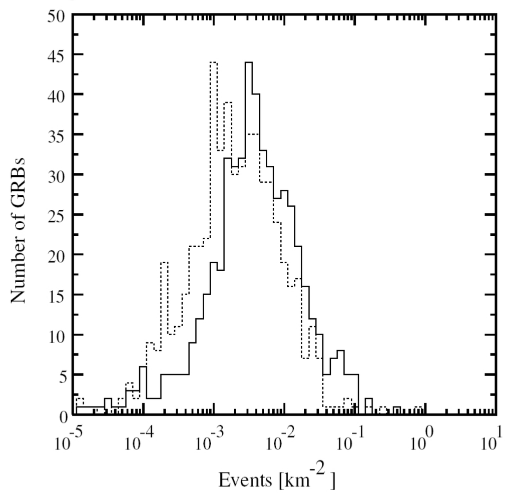

Figure 5 [1] illustrates the distribution of estimated neutrino event rates for discrete long BATSE GRBs. Both distributions have modeled photomeson interactions between fireball protons and prompt synchrotron γ-rays in the internal shocks of the relativistic jet. For the dotted distribution, the proton efficiency (f_π) has been set to 20%, while in the solid distribution, it has been treated as a free parameter (see figure 1). The variance in f_π, which, in conjunction with the fluence, scales the normalization of the neutrino spectrum, can lead to nearly an order of magnitude difference in the neutrino event rate. It is also important to note that very few GRBs are expected to contribute to the possible flux of neutrinos. This underscores the importance of modeling individual bursts for discrete observation, which has been motivated in [1] and is currently being applied to direct AMANDA observations in this work. In the impending era of Swift and IceCube, the rigorous modeling and analysis of discrete GRBs and their observations will help either detect a signal or seriously constrain (and in some cases rule out) models. In this manner, neutrino astronomy can maximize its contribution to the study of GRBs, even in the event of a non-detection.

II. Experimental Techniques: Antarctic Muon and Neutrino Detector Array (AMANDA)

Figure 6: Neutrino Astronomy

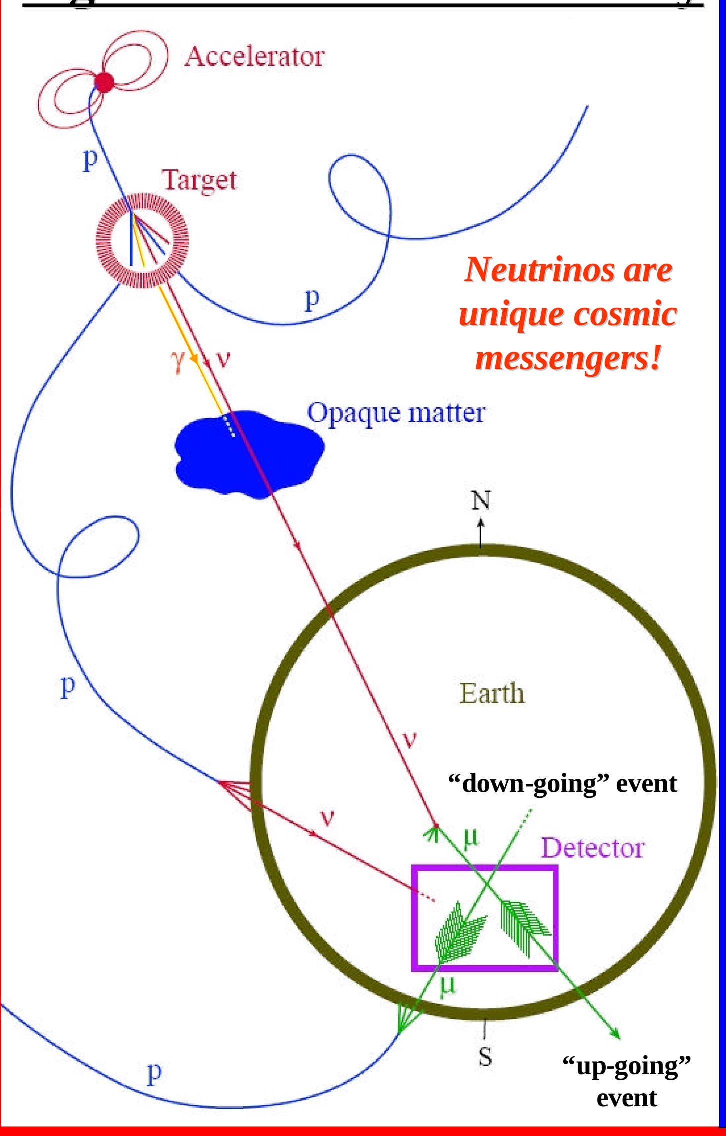

Figure 7: Schematic View

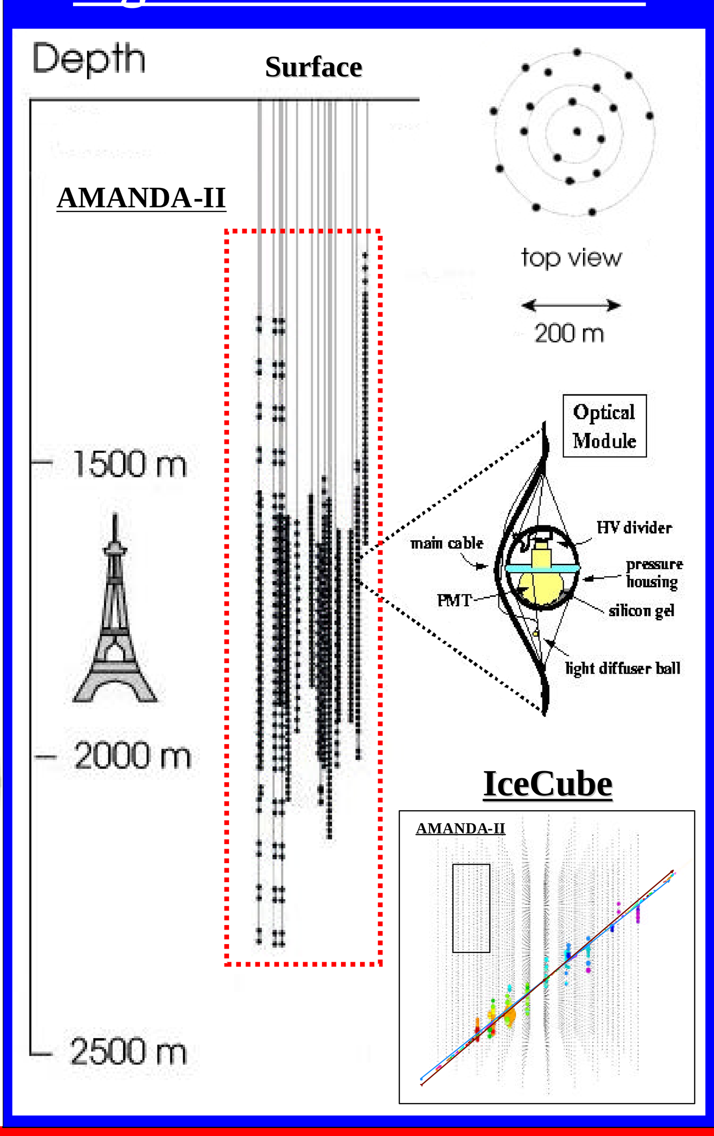

AMANDA: Detection Principles & Reconstruction

- AMANDA is located at the South Pole Station in Antarctica.
- From 1997-1999, AMANDA-B10 was comprised of 10 strings and 302 optical modules (OMs).
- Since 2000, it has been enlarged to 19 strings and 677 OMs and is known as AMANDA-II (see figure 7).
- Charged particles propagating through the ice with velocities > 0.75c will emit Cherenkov Radiation (see figure 8a).
- At AMANDA depths and for λ = 400 nm (maximum OM sensitivity), the average absorption length is ~110 m while the average effective scattering length is ~20 m.
- Neutrino induced muons, via charged current interactions such as: $\nu_\mu + N \rightarrow \mu^\pm + X$, represent signal events which are separated from the background of down-going atmospheric muons (detected at ~ 100 Hz) via the exclusive use of "up-going" muon reconstructed events (see figure 6 & 8b) and selection criteria (quality cuts).
- At TeV energies, the offset between the incident ν_μ and the secondary μ is ~ 1°. The topology and timing of the OM data is used to reconstruct the up-going muon track via a maximum likelihood method to within ~ 2° - 3°.
- Spatial and temporal constraints, in addition to selection parameters are leverage to realize a nearly background-free search [9].

Figure 8: Reconstruction

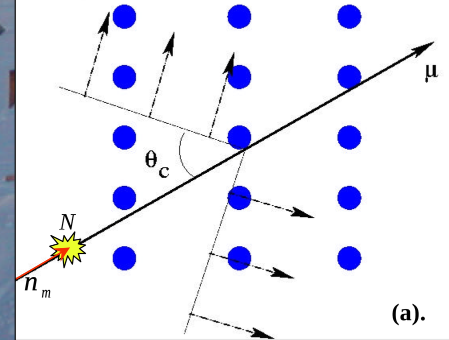

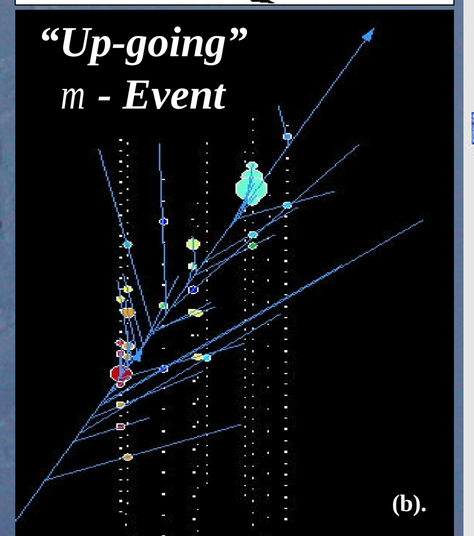

Figure 9: AMANDA-II Effective Muon & Neutrino Areas[9]

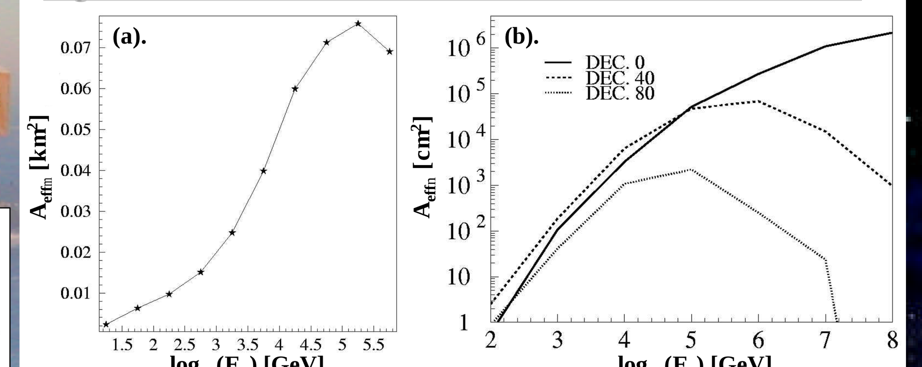

Muon (figure 9a) and neutrino (figure 9b) effective areas [9] for a diffuse GRB - neutrino spectrum [8]. The analysis of over 300 BATSE GRBs has been consistent with no signal, resulting in a preliminary neutrino event upper limit of 1.45 [9]. A full publication is currently in progress.

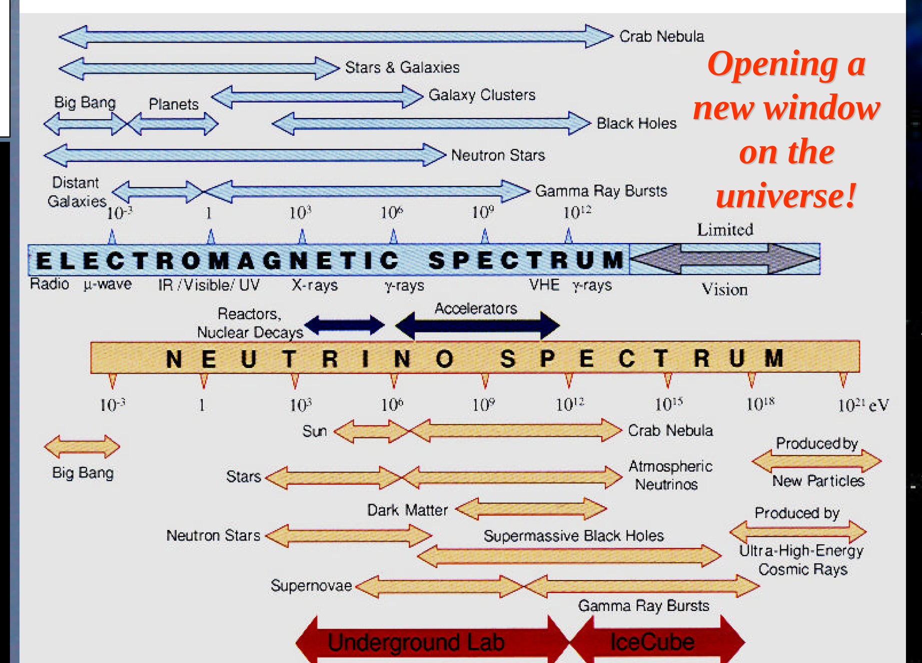

Future Synergy of Neutrino & Gamma Ray Astronomy

These analytical techniques will be implemented in the new era of experimental precision and sensitivity achieved with instruments such as IceCube, Swift and GLAST. The possibility of opening a new chapter of discovery looks very promising.

Neutrino Signal? or Model Constraints?

The enigma continues …

Swift 2004 · GLAST 2007 · IceCube 2005 - 2010 · AMANDA Since 1997

References:

1. Theoretical treatment follows Guetta, D. et al., Astroparticle Physics, 20, 429-455 (2004). For a recent review, see Piran, T. astro-ph/0405503.
2. BATSE Current Catalog *(http://www.batse.msfc.nasa.gov/batse/grb/catalog/current)*.
3. Variability-luminosity redshifts where provided by [1] using the methods described in Fenimore, E. & Ramirez-Ruiz, E. astro-ph/0004176.
4. Lag-luminosity redshifts provided by David Band following the method described in Band, D. et al., astro-ph/0403220.
5. E_P-luminosity redshifts were provided from table 2 of Yonetoku, D. et al., ApJ 609: 935-951 2004 July 10.
6. Spectral fit parameters provided by David Band following the method described in Band, D. L. et al. ApJ: 413, 281 – 292, 1993 August 10.
7. Muniz-Alvarez, J. et al. ApJ 604: L85-L88 2004 April 1.
8. Waxman, E. & Bahcall, J. Phys. Rev. Let. Vol. 78, No. 12, 24 March 1997, Waxman, E. & Bahcall, J. Phys. Rev. D. Vol. 59, 023002.
9. Hardtke, R., Kuehn, K., & Stamatikos, M. "28th ICRC Proceedings," 2003, pp. 2717-2720.

Correspondence to: ms25@amanda.wisc.edu